


Graphyne-oxide supported Pd catalyst with ten times higher nitrobenzenes reduction activity than Pd/C

Bin Wu^{1,2} · Pin Lyu² · Kaixuan Wang^{1,2} · Xiaoyan Qiu² ·
Taifeng Liu² · Fang Zhang² · Hexing Li^{1,2} · Shengxiong Xiao² 

Received: 7 February 2018 / Accepted: 30 May 2018 / Published online: 11 June 2018
© Springer Science+Business Media B.V., part of Springer Nature 2018

Abstract Upon oxidation, a graphyne-like porous carbon-rich network (GYLPC), which is a two-dimensional carbon material consisting of *sp*- and *sp*²-hybridized carbon atoms synthesized via alkyne metathesis reactions, yielded GYLPC oxide (GYLPCO). The highly electron-rich conjugated structure provides this new material GYLPC and its oxide GYLPCO with low reduction potentials, which are found to be able to serve as reductants and stabilizers for electroless deposition of well-dispersed Pd metal nanoparticles. The unique Pd/GYLPCO showed extremely high catalytic activity for a broad scope of nitrobenzene reduction reactions with short reaction time and good yields, even in aqueous media under aerobic conditions. We expect that our approach will further boost research on the design and application of graphyne-like functional materials for catalysis.

Keywords Graphyne-like porous carbon-rich network · Graphyne-like porous carbon-rich network oxide · Nitrobenzene reduction · Pd nanoparticles

Electronic supplementary material The online version of this article (<https://doi.org/10.1007/s11164-018-3492-z>) contains supplementary material, which is available to authorized users.

✉ Hexing Li
hexing-li@shnu.edu.cn

✉ Shengxiong Xiao
senksong@msn.com

¹ School of Chemistry and Molecular Engineering, East China University of Science and Technology, Shanghai 200237, China

² The Education Ministry Key Laboratory of Resource Chemistry, International Joint Laboratory of Resource Chemistry, Shanghai Normal University, Shanghai 200234, China

Introduction

Extensive interests have been drawn to metal nanoparticles because of their numerous applications in various biologically and chemically significant fields [1–3]. And a number of metal nanocatalysts, including Pd, Pt, Au, Cu, Fe, Ni, Ag, Zn and Mn have been developed to catalyze huge numbers of processes in the chemical industry, materials science, nanotechnology, molecular electronics and pharmaceutical sciences [4–6]. To synthesize stable and reactive metal catalysts on the nano scale, metal particles must be produced as small as possible with a high accessible surface area. However, the surface energy increases with decreasing particle size, which usually leads to serious aggregation [7]. To solve this problem, depositing metal nanoparticles onto inert supports is a possible strategy. Besides easier separation and stabilization of metal nanoparticles, the support also plays a key role in promoting catalytic activity by supplying suitable microenvironments of active sites including surface chemistry, coordination models and electron-configuration, etc. [8, 9].

Recently, developing highly efficient and stable supported metal catalysts has become one of the increasingly important goals in chemistry and materials science owing to both economic and environmental reasons [10, 11]. For this purpose, a tremendous amount of researches have been focused upon the uses of sp^2 -hybridized carbon materials as the carrier materials, because they have lower reduction potentials than some kinds of metal ions and could be applied as reductant and stabilizer for electroless deposition of dispersed metal nanoparticles [12, 13]. Electroless deposition is a simple technique that can avoid the use of surfactants or extra reductants or catalysts but have the capability for large-scale production. They could be applied as both the reductant and stabilizer for electroless deposition of metal nanoparticles with high dispersion. As a new carbon allotrope, the graphyne family has been theoretically proposed to possibly feature as assembled layers of sp - and sp^2 -hybridized carbon atoms with striking applications in device and energy materials [14–17]. Recently, a graphyne-like porous carbon-rich network (GYLPC) is synthesized through alkyne metathesis from 1,3,5-tripropynylbenzene [18]. GYLPC comprises benzene rings together with carbon–carbon triple bonds in the structure. Each benzene ring is connected to three adjacent benzene rings through carbon–carbon triple bonds, resulting in a flat porous structure. Carbon–carbon triple bonds with more delocalized π -electrons in GYLPC can result in materials with enriched electron cloud density and enhanced reaction activity. It can be applied as an ideal supporting substrate for depositing metal nanocatalysts [19].

For centuries, Pd-based catalysts have become a hot topic of interest because of their excellent performance in comparison with other catalysts. In general, supported palladium catalysts are prepared by immersing supports in the solution containing palladium ions, followed by reduction into Pd nanoparticles and depositing them into the pore channels and/or onto the surfaces of the supports. Unfortunately, there are many drawbacks which significantly decline the activity of the catalysts. Most of all, the Pd nanoparticles are easy to agglomerate and to be washed away during reaction processing due to the weak Pd-support interaction,

leading to poor catalyst durability. Both the experimental results and theoretical predictions demonstrate that Pd could interact with and bind more strongly to graphdiyne because more interaction states and transmission channels are generated between them [19–21]. Qi et al. [19] investigated electroless deposition to attach palladium nanoparticles into graphdiyne oxide so that the interaction between Pd particles and the support was believed to be stronger.

In this communication, we demonstrate that GYLPC oxide (GYLPCO) can be used for electroless deposition of Pd nanoparticles (NPs) through the direct redox reaction between GYLPCO and PdCl_4^{2-} , in which GYLPCO acts as the reductant and stabilizer. The as-formed Pd/GYLPCO nanocomposite shows extremely high catalytic activity and selectivity toward the reduction of 4-nitrophenol (4-NP) with sodium borohydride (NaBH_4) in aqueous solution at room temperature. Meanwhile, this catalyst displays good tolerance to a variety of different functional groups. Furthermore, various kinds of substituted nitroarenes could also be reduced with very high activities and selectivities.

Results and discussion

The GYLPC used here was synthesized via alkyne metathesis polymerization reaction as reported in our early study [18]. This GYLPC is a novel two-dimensional carbon allotrope consisting of *sp*- and *sp*²-hybridized carbon atoms. Oxidation of GYLPC was performed by acid-oxidation treatment. Briefly, GYLPC powder (20 mg) was first mixed carefully with HNO_3 (6.0 mL), H_2SO_4 (18 mL) and KMnO_4 (60 mg). Then, the mixture was stirred vigorously for 24 h in an oil bath of 80 °C. After being cooled to room temperature, the mixture was subjected to mild ultrasonication for a few minutes, and the pH was adjusted to 8.0 with saturated NaOH solution in water in an ice-bath. The suspension was centrifuged at 9000 rpm for 15 min and washed with deionized water for three times. The resulting precipitate was well-dispersed into water, and the solution was dialyzed (cutoff, 3500) in water for 3 days to give the pure GYLPCO. For comparison, the graphene-oxide supported Pd (Pd/GO), thermally reduced GO supported Pd (Pd/TRGO) and multi-walled carbon nanotube supported Pd (Pd/MWNT) were also prepared. Briefly, 2 mL of aqueous solution containing 0.5 mg/mL dispersed GO, TRGO or MWNTs was mixed with 0.2 mL of aqueous solution containing 10 mM K_2PdCl_4 in an ice-bath and stirred vigorously for 30 min [19]. The resulting catalyst was collected by centrifugation and washing with pure water for several times. Detailed experimental descriptions can be found in the Supporting Information. The Pd/C catalyst was commercially purchased and used without further treatment.

To explore the direct redox reaction property of GYLPCO with PdCl_4^{2-} ion, E_{cutoff} values of GYLPCO were calculated based on ultraviolet photoelectron spectra (UPS, Fig. 1b). The E_{cutoff} value of GYLPCO was determined as 2.49 eV. The work function (Φ) is calculated from the equation of $\Phi = h\nu - E_{\text{Fermi}} + E_{\text{cutoff}}$, where $h\nu$, E_{Fermi} , and E_{cutoff} refer to the photo energy of the excitation light (21.22 eV), the Fermi level edge (19.85 eV in this case), and the inelastic secondary electron cutoff measured in Fig. 1b, respectively. Meanwhile, the reduction

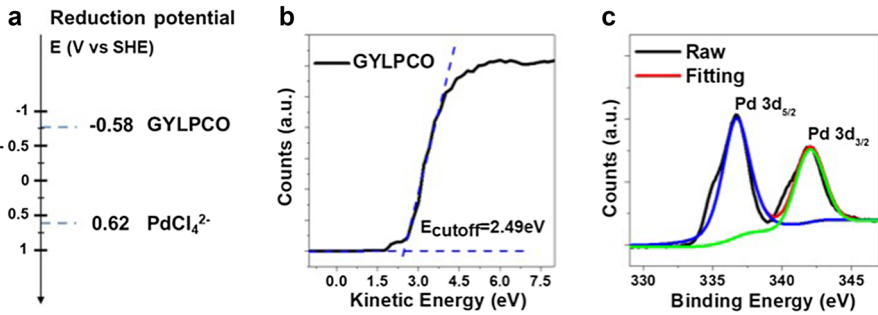


Fig. 1 **a** Schematic reduction potential of PdCl_4^{2-} onto GYLPCO, **b** UPS spectra of GYLPCO, **c** XPS spectra of Pd 3d of Pd/GYLPCO

potential was obtained from the equation of $\Phi/e = E_{\text{vsSHE}} + 4.44$ V, where Φ is the work functions, E is the reduction potential versus standard hydrogen electrode (SHE). The reduction potential of GYLPCO was estimated to be around -0.58 V versus SHE as shown in Fig. 1a, which was close to that of graphdiyne oxide but lower than that of other carbon allotropes such as carbon nanotubes ($+0.50$ V vs. SHE) and graphene oxides ($+0.48$ V vs. SCE), suggesting that GYLPCO was an excellent reducing agent for electroless deposition of metals from the corresponding metallic ions as shown in Fig. 1a.

To demonstrate the electroless deposition of Pd onto GYLPCO, homogeneous suspension of GYLPCO was mixed with an aqueous solution of PdCl_4^{2-} . Then, the mixture was put into an ice bath for 30 min with vigorous stirring. The resulting sample was collected by centrifugation and washing with water for several times. X-ray photoelectron spectroscopy (XPS) spectra demonstrated the presence of Pd, corresponding to the peaks with binding energies around 336.8 and 341.9 eV in $3d_{5/2}$ and $3d_{3/2}$ levels (Fig. 1c). In comparison with the Pd deposited on graphdiyne oxide with Pd $3d_{5/2}$ and Pd $3d_{3/2}$ of 337.4 and 342.7 eV [19], negative shift of binding energies in Pd/GYLPCO was observed. However, the Pd/GYLPCO exhibited positive shift of binding energies compared to Pd deposited on graphene oxide with binding energies of 335.2 and 341.0 eV [22], possibly due to the surface dipole generated by the GYLPCO. Meanwhile, the GYLPCO network of the Pd/GYLPCO was confirmed by the powder X-ray diffraction (XRD) pattern. As shown in Figure S1, the peak ($2\theta = 20.2^\circ$) moved to a smaller angle compared with that in the pure GYLPCO. The d -spacing was increased possibly owing to the existence of C=O and the bonding between Pd NPs and C \equiv C. It did not exhibit any additional peaks indicating that the Pd metal was highly dispersed on the supporting materials [23].

Transmission electron microscopy [24] images in Fig. 2a, b revealed that the as-formed Pd NPs were well dispersed on the surface of GYLPCO with the uniform size of 4.5 ± 0.5 nm. High-resolution transmission electron microscopy (HRTEM) image (Fig. 2b, inset) shows that the interplanar spacing of the Pd particle lattice is 0.221 nm, which agrees well with the (111) lattice spacing of face-centered cubic

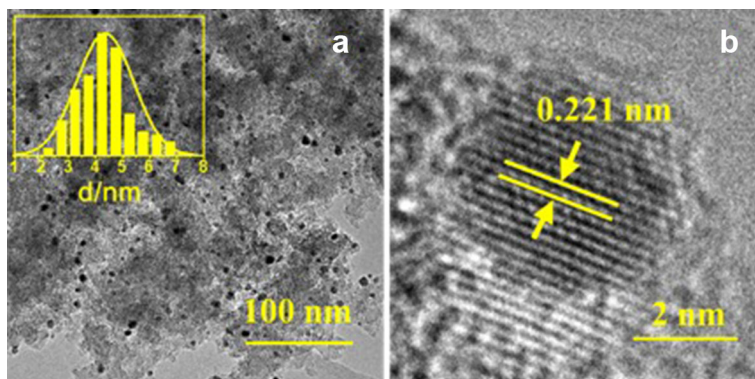


Fig. 2 TEM (a) and HRTEM (b) images of Pd/GYLPCO

Pd (0.224 nm), further confirming the successful electroless deposition of Pd NPs onto the GYLPCO support. Moreover, the results demonstrated here also suggest that GYLPCO could act as stabilizer for Pd NPs, which may be attributed to a strong interaction between Pd nanoparticles and GYLPCO support, presumably owing to the presence of the more active *sp*-hybridized C atoms in the GYLPCO. Such hybridization enables the in-plane p_x - p_y π/π^* orbitals to rotate in any direction perpendicular to the C \equiv C bonds [21]. And it possible for the π/π^* orbitals of the C \equiv C bonds at a given acetylenic ring to point toward the Pd NPs [21], which was similar to the case of graphyne [20] and graphdiyne [25].

The catalytic reduction of nitroarenes to the corresponding amine is popular in organic synthesis because it is one of the atomic-efficient methods for producing intermediates or the key precursors of pharmaceuticals, polymers, pesticides, explosives, fibers, dyes and cosmetics [26, 27]. The reduction of 4-nitrophenol (4-NP) by NaBH_4 was used as a model reaction to investigate the catalytic performance [24, 28]. The aqueous solution of 4-NP itself exhibits a strong absorption peak at 316 nm (Figure S2A). Upon the addition of NaBH_4 into the solution, the absorption peak at 316 nm disappeared along with the appearance of a new peak at 400 nm (Figure S2B) indicative of 4-nitrophenolate ion resulting from 4-NP reduction. And the color of the solution changed from light yellow to bright yellow, which was consistent with the previous report [29, 30]. Upon the addition of Pd/GYLPCO into the mixture of 4-NP and NaBH_4 , the absorption peak at 400 nm decreased rapidly. Meanwhile, a new peak appears at 300 nm characteristic of 4-aminophenol resulted from 4-NP reduction (Figure S2C) [31, 32]. Since the concentration of NaBH_4 was in large excess of 4-NP in the reduction (Figure S3), the reaction was considered as pseudo-first-order with regard to 4-NP only. The determination of the reaction rate was given in Supporting Information (Figure S4). The absorbance was proportional to the concentration of 4-NP in this system, and the value of $\ln(A_t/A_0)$ reflects that of $\ln(C_t/C_0)$, where C_t and C_0 are the concentrations of 4-NP at time t and 0, respectively. Therefore, the reaction rate

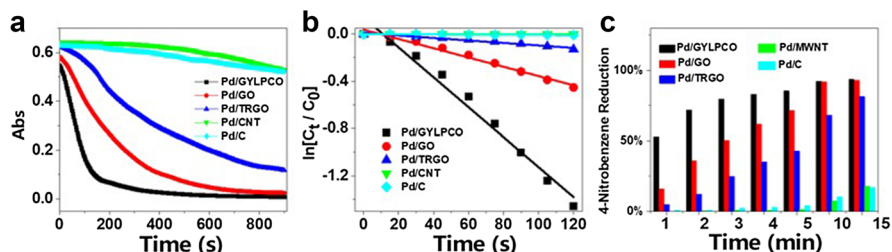
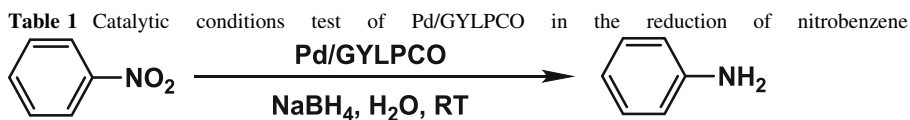


Fig. 3 The reduction of 4-nitrophenol (4-NP) by NaBH_4 catalyzed by five different catalysts of Pd/GYLPCO, Pd/GO, Pd/TRGO (blue), Pd/CNT and commercial Pd/C (cyan). **a** Absorbance (400 nm) versus time, **b** $\ln[C_t/C_0]$ as a function of absorbance (400 nm) versus time, **c** percentage conversion of 4-NP over the course of the reaction (15 min). All the experimental data were repeated five times

constant k was calculated from the rate equation, $\ln[C_t/C_0] = kt$ [33]. To follow the kinetics of the reaction, UV–vis spectra of the reaction mixture were monitored at 3 s intervals regularly. Figure 3a shows the time-dependent UV–vis spectra of 4-NP during its reduction by NaBH_4 on the Pd/GYLPCO catalyst. The rate constant k was calculated to be 0.01266 s^{-1} according to the slope of the fitted line (Fig. 3b, black line). To further investigate into the influence of the supporting materials on the catalytic activity for the reduction of 4-NP, we deposited Pd NPs spontaneously on the surface of other kinds of carbon materials including graphene oxide (GO, C \sim 46 wt%), thermal reduced graphene oxide (TRGO, C \sim 85 wt%) and multi-walled carbon nanotubes (MWNTs) through the redox reaction between PdCl_2^{2-} ion and carbon materials. The rate constant k values were calculated to be 0.00393, 0.00105, 0.00003 and 0.00007 min^{-1} for the Pd/GO, Pd/TRGO, Pd/MWNT, and the commercial Pd/C catalysts, respectively. The rate constant on Pd/GYLPCO was about 3.2-fold higher than that of Pd/GO, 12-fold higher than that of Pd/TRGO, 422-fold higher than that of Pd/MWNT, and 180-fold higher than the commercial Pd/C within 120 s. This difference can be more clearly seen in Fig. 3c. Such excellent catalytic performance of the Pd/GYLPCO could be mainly attributed to synergistic effects from the highly dispersed and surfactant-free nature of Pd clusters benefited from the electroless deposition method and the unique structure of the GYLPCO. These results suggest that smaller size of Pd clusters and larger π -conjugated structure of GYLPCO are mainly responsible for the more efficient catalysis during 4-NP reduction as compared with those of Pd/GO, Pd/MWNT, and commercial Pd/C.

The preliminary studies on the screening showed that the catalyst dosage, temperature and time of reaction had a significant effect on the yields, as shown in Table 1. After optimizations of reaction conditions, the catalytic reduction of nitrobenzene can be finished in a short time (10 min) with excellent yield ($> 99\%$) at room temperature in air using only 0.1 mol% of Pd/GYLPCO catalyst. Also, we



Entry	Catalyst dosage (Pd mol%)	Time (min)	Yield (%)
1	0.50	10	> 99
2	0.25	10	> 99
3	0.10	10	> 99
4	0.05	10	70.4
5	0.10	5	92.3

Reaction conditions: catalyst (Pd 0.50, 0.25, 0.10 or 0.05 mol%), nitroarenes (0.5 mM), NaBH_4 (5 equiv.), water (4 mL), r.t., in air. Yields were determined by LC analysis with mesitylene as internal standard

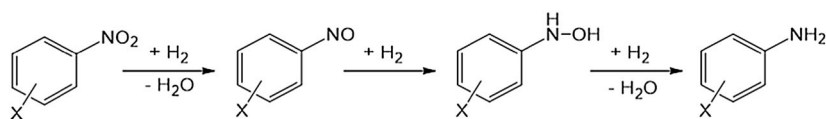
have further extended the Pd/GYLPCO catalyst to various nitroarenes to examine the generality of the reaction. The reaction time and yield of the Pd/GYLPCO-catalyzed reduction of nitroarenes into amines by NaBH_4 in water are summarized in Table 2. For nitrobenzene, aniline is formed with above 99% yield (entry 1). The reactions of substrates bearing an electron-donating group (*ortho*-, *meta*- or *para*-substitution site) produce the corresponding products in excellent yields (entries 2–10). In fact, some of the nitroarenes with a strong electron-donating group completed in just a few minutes (entries 4–5). In addition, electron-withdrawing groups like carbonyl functionalities in nitroarenes remain intact when using the Pd/GYLPCO catalyst (entry 11–12). And the intermediate *N*-hydroxylaniline is clearly observed with a certain amount of Pd/GYLPCO catalysts in our case (Figure S5). According to the observations described above, we propose a general mechanistic pathway for the Pd-catalyzed reduction of nitroarenes (Scheme 1) [34–36]. The reduction of nitroarenes by NaBH_4 with other supported metal catalysts could yield aromatic amines [37, 38] through different intermediate processes [39–41]. While in our case, the reduction of nitroarenes into amines on our Pd/GYLPCO catalysts is close to nearly 99%. Even in the presence of some other substrates, we also got relatively high activities and yields. It can be attributed to the strong metal-support interaction (SMSI) [42], the *d*- π conjunctions [43] and the unique interfacial electronic effect [44], which derive from in-plane π/π^* orbitals to rotate in any direction perpendicular to the line of the $\text{C}\equiv\text{C}$ bonds in the GYLPCO. The electron-rich Pd/GYLPCO surface could possibly alter the electron state of nitrobenzenes thus to enhance the activity.

Table 2 Catalytic reduction of nitroarenes into amines by NaBH_4 catalyzed by Pd/GYLPCO

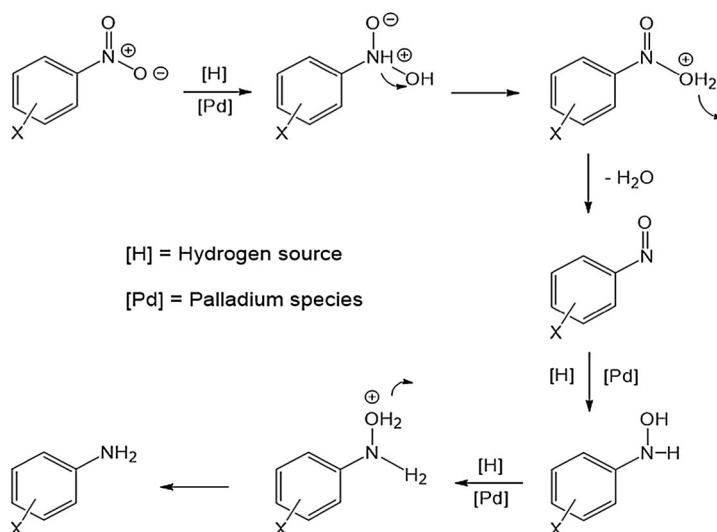
entry	Reactant	Product	Time (min)	Yield (%)
1			10	>99
2			10	>99
3			10	>99
4			5	>99
5			5	>99
6			10	>99
7			10	>99
8			10	>99
9			10	95.8
10			20	78.6
11			20	90.3
12			20	86.4

Reaction conditions: catalyst (Pd 0.1 mol%), nitroarenes (0.5 mM), NaBH_4 (5 equiv.), water (4 mL), r.t., in air. Yields were determined by LC analysis with mesitylene as internal standard

A direct pathway:



A possible reaction mechanism



Scheme 1 Proposed mechanism for the reduction of nitroarenes using NaBH_4 catalyzed by Pd/GYLPCO

Conclusion

In summary, we have demonstrated for the first time that GYLPCO can be used as the reductant and stabilizer for electroless deposition of highly dispersed and surfactant-free Pd clusters owing to its low reduction potential and highly conjugated electronic structure. Further, GYLPCO, the oxidation form of GYLPC, is observed to be an even excellent substrate for depositing ultrafine Pd clusters to form Pd/GYLPCO nanocomposite which shows a high catalytic performance toward the reduction of nitroarenes. The high performance could be considered to arise from synergetic effects that occur at the Pd/GYLPCO nanocomposite. This work is believed to be significantly beneficial to the design and development of active supported metal catalysts, which could serve as advanced catalytic systems for practical applications.

Acknowledgements We acknowledge financial support from the National Natural Science Foundation of China (Nos. 21473113, 21772123 and 51502173), Program for Professor of Special Appointment (Eastern Scholar) at Shanghai Institutions of Higher Learning (No. 2013-57), “Shuguang Program” supported by Shanghai Education Development Foundation and Shanghai Municipal Education Commission (14SG40), Program of Shanghai Academic/Technology Research Leader (No.

16XD1402700), National Natural Science Foundation of Shanghai (No. 15ZR1431100), Ministry of Education of China (PCSIRT_16R49) and International Joint Laboratory of Resource Chemistry (IJLRC).

Compliance with ethical standards

Conflict of interest The authors declare that they have no conflict of interest.

References

1. L. Wang, F.-S. Xiao, *Green Chem.* **17**, 24 (2015)
2. J. Huang, L. Lin, D. Sun, H. Chen, D. Yang, Q. Li, *Chem. Soc. Rev.* **44**, 6330 (2015)
3. W.J. Stark, P.R. Stoessel, W. Wohlleben, A. Hafner, *Chem. Soc. Rev.* **44**, 5793 (2015)
4. Y.-B. Huang, J. Liang, X.-S. Wang, R. Cao, *Chem. Soc. Rev.* **46**, 126 (2017)
5. K.S. Egorova, V.P. Ananikov, *Angew. Chem. Int. Ed.* **55**, 12150 (2016)
6. K.D. Gilroy, A. Ruditskiy, H.-C. Peng, D. Qin, Y. Xia, *Chem. Rev.* **116**, 10414 (2016)
7. R.J. White, R. Luque, V.L. Budarin, J.H. Clark, D.J. Macquarrie, *Chem. Soc. Rev.* **38**, 481 (2009)
8. C.T. Campbell, *Acc. Chem. Res.* **46**, 1712 (2013)
9. M. Cargnello, V.V.T. Doan-Nguyen, T.R. Gordon, R.E. Diaz, E.A. Stach, R.J. Gorte, P. Fornasiero, C.B. Murray, *Science* **341**, 771 (2013)
10. L.-B. Sun, X.-Q. Liu, H.-C. Zhou, *Chem. Soc. Rev.* **44**, 5092 (2015)
11. J.D.A. Pelletier, J.-M. Basset, *Acc. Chem. Res.* **49**, 664 (2016)
12. P.R. Unwin, A.G. Güell, G. Zhang, *Acc. Chem. Res.* **49**, 2041 (2016)
13. L. He, F. Weniger, H. Neumann, M. Beller, *Angew. Chem. Int. Ed.* **55**, 12582 (2016)
14. N. Wang, J. He, Z. Tu, Z. Yang, F. Zhao, X. Li, C. Huang, K. Wang, T. Jiu, Y. Yi, Y. Li, *Angew. Chem. Int. Ed.* **56**, 10740 (2017)
15. S. Zhang, H. Du, J. He, C. Huang, H. Liu, G. Cui, Y. Li, *ACS Appl. Mater. Interfaces* **8**, 8467 (2016)
16. H. Du, H. Yang, C. Huang, J. He, H. Liu, Y. Li, *Nano Energy* **22**, 615 (2016)
17. Y. Li, J. Tang, X. Cui, J. Lee, *Acta Phys. Chim. Sin.* **34**, 1080 (2018)
18. B. Wu, M. Li, S. Xiao, Y. Qu, X. Qiu, T. Liu, F. Tian, H. Li, S. Xiao, *Nanoscale* **9**, 11939 (2017)
19. H. Qi, P. Yu, Y. Wang, G. Han, H. Liu, Y. Yi, Y. Li, L. Mao, *J. Am. Chem. Soc.* **137**, 5260 (2015)
20. P. Wu, P. Du, H. Zhang, C. Cai, *Phys. Chem. Chem. Phys.* **17**, 1441 (2015)
21. D.W. Ma, T. Li, Q. Wang, G. Yang, C. He, B. Ma, Z. Lu, *Carbon* **95**, 756 (2015)
22. X. Chen, G. Wu, J. Chen, X. Chen, Z. Xie, X. Wang, *J. Am. Chem. Soc.* **133**, 3693 (2011)
23. W. Xu, X. Liu, J. Ren, P. Zhang, Y. Wang, Y. Guo, Y. Guo, G. Lu, *Catal. Commun.* **11**, 721 (2010)
24. M. Gholinejad, F. Zareh, C. Nájera, *Appl. Organomet. Chem.* **32**, e3984 (2017)
25. J. He, S.Y. Ma, P. Zhou, C.X. Zhang, C. He, L.Z. Sun, *J. Phys. Chem. C* **116**, 26313 (2012)
26. F. Yang, C. Chi, C. Wang, Y. Wang, Y. Li, *Green Chem.* **18**, 4254 (2016)
27. H. Goksu, H. Sert, B. Kilbas, F. Sen, *Curr. Org. Chem.* **21**, 794 (2017)
28. R. Nazir, P. Fägeria, M. Basu, S. Gangopadhyay, S. Pande, *New J. Chem.* **41**, 9658 (2017)
29. Y. Deng, Y. Cai, Z. Sun, J. Liu, C. Liu, J. Wei, W. Li, C. Liu, Y. Wang, D. Zhao, *J. Am. Chem. Soc.* **132**, 8466 (2010)
30. J. Ge, Q. Zhang, T. Zhang, Y. Yin, *Angew. Chem. Int. Ed.* **47**, 8924 (2008)
31. Y. Dai, S.J. Liu, N.F. Zheng, *J. Am. Chem. Soc.* **136**, 5583 (2014)
32. N. Lu, W. Chen, G.Y. Fang, B. Chen, K.Q. Yang, Y. Yang, Z.C. Wang, S.M. Huang, Y.D. Li, *Chem. Mater.* **26**, 2453 (2014)
33. K. Halder, G. Bengtson, V. Filiz, V. Abetz, *Appl. Catal. A Gen.* **555**, 178 (2018)
34. Y.-J. Kim, R. Ma, D.A. Reddy, T.K. Kim, *Appl. Surf. Sci.* **357**, 2112 (2015)
35. S. Mahata, A. Sahu, P. Shukla, A. Rai, M. Singh, V.K. Rai, *New J. Chem.* **42**, 2067 (2018)
36. S. Doherty, J.G. Knight, T. Backhouse, A. Bradford, F. Saunders, R.A. Bourne, T.W. Chamberlain, R. Stones, A. Clayton, K. Lovelock, *Catal. Sci. Technol.* **8**, 1454 (2018)
37. R.V. Jagadeesh, A.E. Surkus, H. Junge, M.M. Pohl, J. Radnik, J. Rabeah, H.M. Huan, V. Schunemann, A. Bruckner, M. Beller, *Science* **342**, 1073 (2013)
38. Z.Z. Wei, J. Wang, S.J. Mao, D.F. Su, H.Y. Jin, Y.H. Wang, F. Xu, H.R. Li, Y. Wang, *ACS Catal.* **5**, 4783 (2015)

39. A. Corma, P. Concepcion, P. Serna, *Angew. Chem. Int. Ed.* **46**, 7266 (2007)
40. H. Wiener, J. Blum, Y. Sasson, *J. Org. Chem.* **56**, 4481 (1991)
41. K. Shimizu, Y. Miyamoto, T. Kawasaki, T. Tanji, Y. Tai, A. Satsuma, *J. Phys. Chem. C* **113**, 17803 (2009)
42. P. Serna, A. Corma, *ACS Catal.* **5**, 7114 (2015)
43. Z. Lu, S. Li, P. Lv, C. He, D. Ma, Z. Yang, *Appl. Surf. Sci.* **360**, 1 (2016)
44. G. Chen, C. Xu, X. Huang, J. Ye, L. Gu, G. Li, Z. Tang, B. Wu, H. Yang, Z. Zhao, Z. Zhou, G. Fu, N. Zheng, *Nat. Mater.* **15**, 564 (2016)